GEOPHYSICAL RESEARCH LETTERS, VOL. 27, NO. 19, PAGES 3045-3048, OCTOBER 1, 2000

Precipitation changes in a GCM resulting from the indirect effects of anthropogenic aerosols

Leon D. Rotstayn and Brian F. Ryan

CSIRO Atmospheric Research, Aspendale, Victoria, Australia

Joyce E. Penner

Department of Atmospheric, Oceanic and Space Sciences, University of Michigan, Ann Arbor

Abstract. An atmospheric GCM coupled to a mixed-layer ocean model is used to study changes in rainfall due to the indirect effects of anthropogenic aerosols. The model includes treatments of both the first and second indirect effects. The most striking feature of the equilibrium rainfall response to the indirect effects of anthropogenic aerosols is a southward shift of the equatorial rainfall. We hypothesize that this is caused by a hemispheric asymmetry in the cooling of the sea surface. This is supported by another pair of experiments, in which the model is run with prescribed present-day SSTs. In one experiment the standard model is used, and in the other the SSTs in the Northern Hemisphere are increased by 1 K in the calculation of the surface fluxes, to mimic the effect of a return to pre-industrial conditions. Compared to the run with increased NH SST, the standard run shows a southward shift of equatorial rainfall, similar to that obtained as a response to anthropogenic aerosols.

1. Introduction

Sulfates and other aerosols act as cloud condensation nuclei (CCN), so anthropogenic aerosols are thought to increase the cloud-droplet number concentration N_d in liquid-water clouds. The impact of the first indirect aerosol effect, the increase in cloud optical depth that results from these anthropogenic increases in N_d [*Twomey*, 1977], has been extensively studied using global climate models (GCMs). However, the second indirect effect, the suppression of rainfall due to anthropogenic increases in N_d [*Albrecht*, 1989], has been considered in relatively few such studies. Observational evidence for regional reductions in rainfall due to anthropogenic aerosols was presented more than 30 years ago by *Warner* [1968], and more recently by *Rosenfeld* [2000], so it is of interest to consider such changes as simulated in GCMs. A few authors [*Lohmann and Feichter*, 1997; *Rotstayn*, 1999; *Lohmann et al.*, 2000; *Ghan et al.*, 2000] have used GCMs to calculate the radiative forcing due to the indirect aerosol effect, but did not calculate the climatic response or the simulated changes in rainfall. *Meehl et al.* [1996] and *Roeckner et al.* [1999] included the indirect effect in transient climate-change experiments performed with coupled GCMs, but only in conjuction with changes in CO_2, and their models did not include the second indirect effect. *LeTreut et al.* [1998] calculated the climatic response of their GCM to the indirect aerosol effect, but did not show the changes in rainfall. In this paper, we focus on the rainfall changes simulated by a GCM that includes a link between the distribution of aerosol and cloud-droplet concentration, which then affects the cloud-radiative properties and the initiation of rainfall.

Paper number 2000GL011737.
0094-8276/00/2000GL011737$05.00

2. Model and Experiments

We use a low-resolution (spectral R21) version of the CSIRO GCM, with 18 vertical levels. The model includes a physically based treatment of stratiform clouds and precipitation, and interactive calculation of cloud-radiative properties [*Rotstayn*, 1997]. The dependence of rain formation on N_d enters through the parameterization of autoconversion in stratiform clouds. Autoconversion is suppressed until the mixing ratio of cloud liquid water reaches a critical value

$$q_{\rm crit} = \frac{4}{3}\pi\rho_l r_{\rm crit}^3 N_d/\rho, \qquad (1)$$

where $r_{\rm crit} = 9.3$ μm is a prescribed critical cloud droplet radius, ρ_l is the density of liquid water, and ρ is the air density. We use a modification of the autoconversion treatment [*Rotstayn*, 2000], whereby the assumed sub-grid distribution of moisture used by the condensation scheme is used to calculate the fraction of the cloudy area in a grid box in which the local liquid-water mixing ratio exceeds $q_{\rm crit}$. Autoconversion then occurs in this fraction of the cloudy area. The autoconversion rate varies as $N_d^{-1/3}$, but it is the linear dependence of $q_{\rm crit}$ on N_d through (1) that effectively controls the response of the model to changes in N_d.

In common with other convection schemes used in GCMs, the model's mass-flux convection scheme [*Gregory and Rowntree*, 1990] includes only a simple treatment of the microphysics of rainfall generation. Once a critical cloud depth (which differs for land and ocean points) is reached, liquid water in excess of a prescribed threshold falls out of the updraft. There is no dependence of this threshold on the distribution of aerosols. In other words, we consider the second indirect effect only for stratiform clouds.

As in several other studies, N_d is estimated empirically from the mass concentration of sulfate [*Boucher and Lohmann*, 1995]. This means that sulfate is used as a surrogate for all aerosols that act as CCN, assuming that the fraction of sulfate in aerosols remains constant. Such a treatment is appropriate for aerosols from industrial regions, since the parameterization is based on measurements in regions impacted by industrial aerosols, but may not apply to aerosols from biomass burning. The sulfate concentration is

Table 1. Details of experiments and selected global-mean quantities

Experiment	N_d in autoconversion	N_d in radiation	direct aerosol	surface air temperature	precipitation	stratiform precipitation
MLO_PD_ALL	PD	PD	PD	287.13	2.89	0.86
MLO_PI_RAIN	PI	PD	PD	288.33	3.06	0.92
MLO_PI_RAD	PD	PI	PD	288.35	2.99	0.87
MLO_PI_DIR	PD	PD	PI	287.81	2.95	0.87
MLO_PI_ALL	PI	PI	PI	290.01	3.21	0.93

PD denotes present-day; PI denotes pre-industrial. Surface air temperature in Kelvin, precipitation and stratiform precipitation in mm day^{-1}.

obtained from monthly mean distributions of sulfate column burden generated by a chemical transport model [*Penner et al.*, 1994]. These distributions were shown by *Rotstayn* [1999], who found that the cloud-droplet effective radii generated by the model agreed quite well with satellite-retrieved values. A simple treatment of the direct radiative effect of sulfate, which entails a perturbation of the surface albedo, is also included in the model.

Details of the experiments are given in Table 1, together with some key global-mean quantities. The distribution of sulfate used to derive N_d for input to the autoconversion and/or radiation schemes was varied between one applicable to present-day (PD) conditions and one applicable to pre-industrial (PI) conditions. The sea-surface temperatures (SSTs) were obtained from a mixed-layer ocean model with prescribed heat transports. In each experiment, the model was initialized from a July 1 condition saved from a run forced by prescribed PD SSTs. It was run to equilibrium in each case, and then for another 10 years, for which period the model statistics were saved. The equilibration period was 16.5 years for the MLO_PD_ALL run, increasing to a maximum of 41.5 years for the MLO_PI_ALL run, which had the largest perturbation relative to PD conditions. These experiments allow the rainfall to respond to changes in circulation due to the radiative effects of changes in cloud properties and the resulting changes in SST.

3. Results and discussion

Figure 1 shows the global distribution of precipitation, annually averaged from the MLO_PD_ALL run, together with an observed distribution for the period July 1987 to December 1994 [*Huffman et al.*, 1997]. The model successfully captures the broad features of the distribution of precipitation for the present climate. The inter-tropical convergence zone (ITCZ) over the Pacific is well defined, especially in view of the low resolution of the model.

Global-mean values of the surface air temperature, precipitation and stratiform precipitation from each run are given in Table 1. Although the temperature change is similar for the first (MLO_PD_ALL minus MLO_PI_RAD) and second (MLO_PD_ALL minus MLO_PI_RAIN) indirect effects, there is a larger change in precipitation due to the second effect, seen mainly in the stratiform component. This suggests that the model is giving a decrease in precipitation due to the microphysical suppression of stratiform rainfall, as well as a separate decrease due to an overall weakening of the hydrological cycle in the cooler climate. The surface coolings given in Table 1 (e.g., 2.9 K for the total aerosol effect) are substantial compared to the warming of 3.6 K given by the model for a doubling of CO_2. The global-mean radiative forcing of -2.6 W m^{-2} given by this version of the CSIRO GCM for the total indirect aerosol effect is well within the range of results obtained using other models that include the second indirect effect, but may be too large to reconcile with the observed warming to date. Thus, the model may also tend to exaggerate the magnitude of changes in the hydrological cycle.

Figure 2a shows the difference in precipitation between the MLO_PD_ALL and MLO_PI_RAIN runs, that is, the change due to the second indirect effect. The most striking feature is the southward shift of the rainfall in the ITCZ, especially over the Pacific Ocean. Outside of the tropics, the changes are smaller, although some of the more polluted

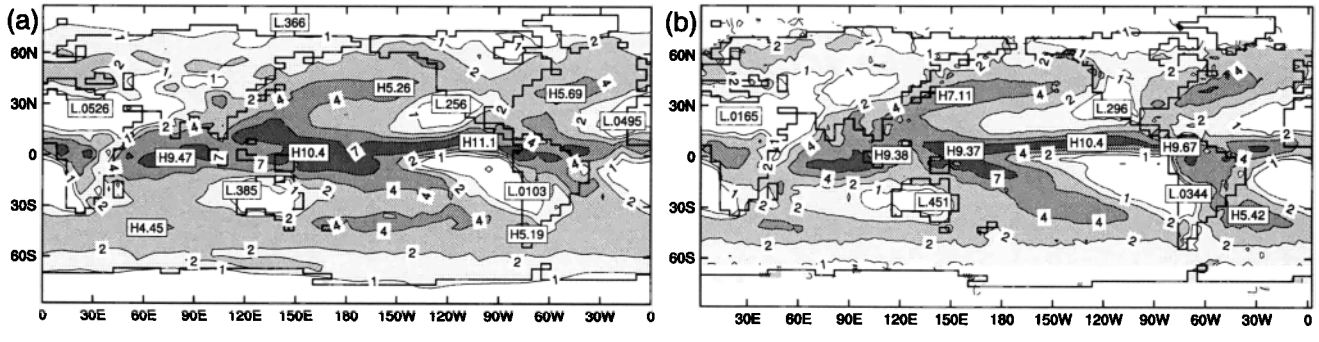

Figure 1. Annual-mean precipitation (a) from the MLO_PD_ALL simulation, and (b) from observations *Huffman et al.* [1997]. Contours are 1, 2, 4, 7 and 10 mm per day.

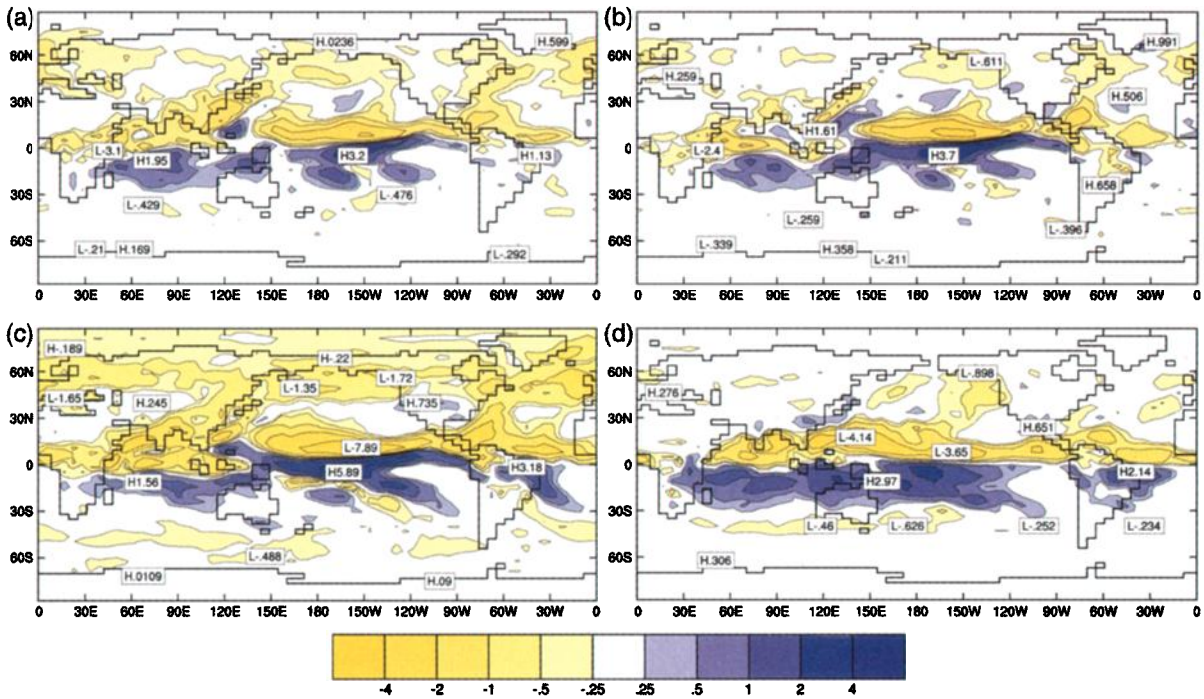

Figure 2. Differences in annual-mean precipitation (a) between the MLO_PD_ALL and MLO_PI_RAIN simulations (the second indirect effect), (b) between the MLO_PD_ALL and MLO_PI_RAD simulations (the first indirect effect), (c) between the MLO_PD_ALL and MLO_PI_ALL simulations (the total aerosol effect), and (d) between the FIXED_PD_ALL and FIXED_PD_NH+1 simulations (the effect of an imposed 1 K, hemispheric asymmetry in SST). Contours are ± 0.25, 0.5, 1, 2 and 4 mm per day.

regions in the Northern Hemisphere (NH) have reductions that exceed 0.5 mm per day. The large tropical changes must be mostly caused by changes in the atmospheric circulation, because the rainfall there is dominated by the convective component. Figure 2b shows the difference in precipitation between the MLO_PD_ALL and MLO_PI_RAD runs, that is, the change resulting from the first indirect effect. In the tropics, the pattern is similar to that in Fig. 2a, confirming that the rainfall changes there are dynamically driven. In the more polluted regions of the NH, the reductions in precipitation are smaller than those in Fig. 2a, suggesting that the microphysical suppression of rainfall due to the second indirect effect may be significant there. Figure 2c shows the difference in precipitation between the MLO_PD_ALL and MLO_PI_ALL runs, that is, the result of the total aerosol effect. In this case the tropical pattern is similar, except that the magnitudes of the changes are larger than those due to the indirect effects alone. The rainfall response to the direct effect alone is similar in pattern, but relatively weak (not shown). Note that the rainfall changes due to the radiative-dynamical response of the model are much larger than any changes due to the purely microphysical suppression of stratiform rainfall by the second indirect effect.

Figure 3 shows that both indirect effects result in a larger reduction of SST in the NH than in the SH. This effect is magnified when the total effect of aerosols is considered. The SST asymmetry gives a corresponding asymmetry in surface evaporation. For example, the reduction in evaporation from the sea surface due to the total aerosol effect is 0.37 mm per day in the NH, but only 0.17 mm per day in the SH.

We hypothesize that the simulated southward shift of the rainfall in the ITCZ is caused by this hemispheric asymmetry in the surface cooling. To isolate this effect,we compared a 10-year simulation of the present climate using fixed monthly mean SSTs (FIXED_PD_ALL) with an otherwise identical run (FIXED_PD_NH+1) in which the SSTs in the NH were increased by 1 K in the calculation of the surface fluxes, to crudely mimic the effect of a return to PI aerosols. Relative to the FIXED_PD_NH+1 run, the FIXED_PD_ALL run showed a southward shift of the rainfall in the ITCZ (Fig. 2d). The shift is remarkably similar to the response obtained from the indirect aerosol effect, thus supporting our hypothesis. As well as a reduction in precipitation north of the equator, there is a corresponding increase in precipita-

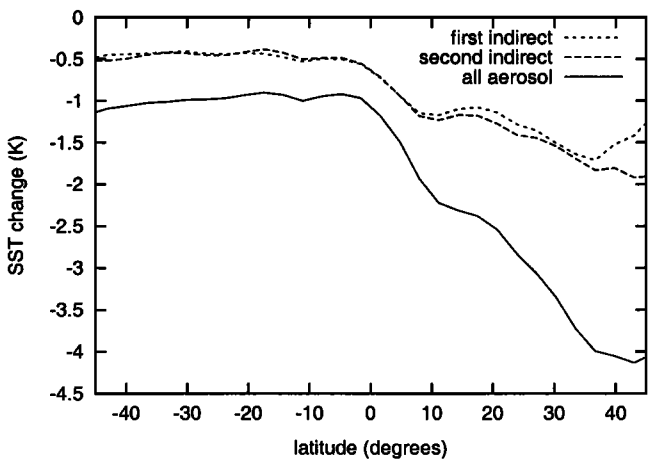

Figure 3. Differences in zonal-mean equilibrium SST from 45°S to 45°N, between the MLO_PD_ALL and MLO_PI_RAD simulations (first indirect effect), the MLO_PD_ALL and MLO_PI_RAIN simulations (second indirect effect) and the MLO_PD_ALL and MLO_PI_ALL simulations (all aerosol effects)

tion south of the equator, suggesting that there is competition between the two upward branches of the Hadley cell. The surface evaporation is a strong function of SST, so we performed a further run, identical to the FIXED_PD_ALL run, except that the surface evaporation from the ocean surface in the NH was increased by 20%, to again crudely mimic the effect of a return to PI aerosols. Relative to this run, the FIXED_PD_ALL run again gave a southward shift of the rainfall in the ITCZ (not shown), suggesting that a hemispheric asymmetry in surface evaporation is itself an important factor.

The details of the rainfall response we found should be viewed with caution. Important limitations are the empirical method used to parameterize N_d, the low resolution of our model, the use of a mixed-layer ocean model (which assumes that the oceanic heat transports remain fixed under climate change), the use of monthly mean sulfate distributions rather than a fully interactive sulfur cycle, and (in common with other GCMs) the need to use simplified representations of many key microphysical processes. Also in common with other GCMs, there is no link between aerosols and the properties of ice clouds, principally because this link is not yet well understood. However, in view of the strong response that we obtained in the Pacific, we believe it is important to further investigate the rainfall response using fully coupled models, together with more physically based treatments of cloud-droplet nucleation. The response to projected future changes in aerosols should also be investigated, as emissions are increasing rapidly in south-east Asia.

References

Albrecht, B. A., Aerosols, cloud microphysics, and fractional cloudiness, *Science*, *245*, 1227–1230, 1989.

Boucher, O., and U. Lohmann, The sulfate-CCN-cloud albedo effect. A sensitivity study with two general circulation models, *Tellus*, *47B*, 281–300, 1995.

Ghan, S., R. Easter, E. C. H. Abdul-Razzak, Y. Zhang, L. Leung, N. Laulainen, R. Saylor, and R. Zaveri, A physically-based estimate of radiative forcing by anthropogenic sulfate aerosol, *J. Geophys. Res.*, in press, 2000.

Gregory, D., and P. R. Rowntree, A mass flux convection scheme with representation of cloud ensemble characteristics and stability-dependent closure, *Mon. Weather Rev.*, *118*, 1483–1506, 1990.

Huffman, G. J., R. F. Adler, P. A. Arkin, A. Chang, R. Ferraro, A. Gruber, J. Janowiak, R. J. Joyce, A. McNab, B. Rudolf, and U. Schneider, The Global Precipitation Climatology Project (GPCP) combined precipitation dataset, *Bull. Amer. Meteorol. Soc.*, *78*, 5–20, 1997.

Le Treut, H., M. Forichon, O. Boucher, and Z.-X. Li, Sulfate aerosol indirect effect and CO_2 greenhouse forcing: Equilibrium response of the LMD GCM and associated cloud feedbacks, *J. Clim.*, *11*, 1673–1684, 1998.

Lohmann, U., and J. Feichter, Impact of sulfate aerosols on albedo and lifetime of clouds: A sensitivity study with the ECHAM4 GCM, *J. Geophys. Res.*, *102*, 13685–13700, 1997.

Lohmann, U., J. Feichter, J. E. Penner, and R. Leaitch, Indirect effect of sulfate and carbonaceous aerosols: A mechanistic treatment, *J. Geophys. Res.*, *105*, 12,193–12,206, 2000.

Meehl, G. A., W. M. Washington, D. J. Erickson III, and B. P. Briegleb, Climate change from increased CO_2 and direct and indirect effects of sulfate aerosols, *Geophys. Res. Lett.*, *23*, 3755–3758, 1996.

Penner, J. E., C. A. Atherton, and T. E. Graedel, Global emissions and models of photochemically active compounds, in *Global Atmospheric-Biospheric Chemistry*, ed. R. Prinn, pp. 223–248, Plenum, New York, 1994.

Roeckner, E., L. Bengtsson, J. Feichter, L. Lelieveld, and H. Rohde, Transient climate change simulations with a coupled atmosphere-ocean GCM including the tropospheric sulfur cycle, *J. Clim.*, *12*, 3004–3032, 1999.

Rosenfeld, D., Suppression of rain and snow by urban and industrial air pollution, *Science*, *287*, 1793–1796, 2000.

Rotstayn, L. D., A physically based scheme for the treatment of stratiform clouds and precipitation in large-scale models. I: Description and evaluation of the microphysical processes, *Q. J. R. Meteorol. Soc.*, *123*, 1227–1282, 1997.

Rotstayn, L. D., Indirect forcing by anthropogenic aerosols: A global climate model calculation of the effective-radius and cloud-lifetime effects, *J. Geophys. Res.*, *104*, 9369–9380, 1999.

Rotstayn, L. D., On the "tuning" of autoconversion parameterizations in climate models, *J. Geophys. Res.*, *105*, 15,495–15,507, 2000.

Twomey, S., The influence of pollution on the shortwave albedo of clouds, *J. Atmos. Sci.*, *34*, 1149–1152, 1977.

Warner, J., A reduction in rainfall associated with smoke from sugar-cane fires – An inadvertent weather modification, *J. Appl. Meteorol.*, *7*, 247–251, 1968.

L. D. Rotstayn and B. F. Ryan, CSIRO Atmospheric Research, PB1, Aspendale, Vic., 3195, Australia. (e-mail: leon.rotstayn@dar.csiro.au)

J. E. Penner, Department of Atmospheric, Oceanic and Space Sciences, University of Michigan, 2455 Hayward, Ann Arbor, MI, 48109. (e-mail: penner@umich.edu)

(Received March 23, 2000;accepted July 26, 2000)